Quality Improvement of Video over UMTS by Estimating the Velocity of the Mobile Terminal

Stephan Saur and Joachim Speidel
Institut für Nachrichtenübertragung, Universität Stuttgart

Abstract

One challenge of beyond 3G systems are applications with high demands on the quality of service. Transmission and reception of video in a moving car are prominent examples. We present a receiver which estimates the velocity of the mobile terminal for the Universal Terrestrial Radio Access (UTRA) uplink connection in Frequency Division Duplex (FDD) mode. In contrast to a receiver with conventional estimation of the time-variant mobile radio channel with multiple propagation paths, we have designed a channel estimator, which adapts to the estimated velocity. Parameters are optimized for a wide range of speeds. It is shown that the proposed receiver can reduce the block error ratio (BLER) significantly even for high speed of the mobile terminal compared to conventional solutions.

1 Introduction

Due to reflections, diffractions and scattering in a radio channel, the signal propagates on multiple paths. In addition the terminal is moving. Consequently the mobile radio channel is time-variant. Therefore, channel estimation is an essential function of the receiver.
Each UMTS radio uplink is equipped with a Dedicated Physical Control Channel (DPCCH) that contains a pilot pattern which may be utilized at the receiver for channel estimation and signal-to-interference ratio (SIR) estimation. The DPCCH is code multiplexed with the user data (DPDCH). Thus a certain portion of the entire transmit power is reserved for control information.
In section 2 the time-variant mobile radio channel model with multipath propagation that we use for simulation is described. Also a brief description of the 3GPP compliant transmitter of a mobile terminal and the receiver of a UMTS base station is presented.
The quality of the channel estimates has significant impact on the bit error ratio (BER) and the block error ratio (BLER). For channel estimation the Weighted-Multi-Slot-Averaging (WMSA) algorithm is used. It is presented in section 3. The impact of the mobile terminal's velocity on the estimates is shown by some examples.
With knowledge of the velocity the channel estimator can adapt its parameters. Thus, the quality of channel estimation is improved significantly. One basic method for velocity estimation in the frequency domain is presented in section 4.
The BLER of the receiver with velocity estimation is compared to the conventional method in section 5.
Finally, in section 6 we summarize the most important results.

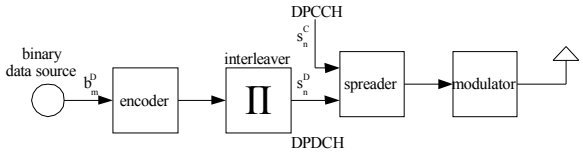

Figure 1: 3GPP conform transmitter of a mobile terminal

2 System Model

2.1 Transmitter

Figure 1 shows the transmitter which consists of the binary data source with information bits b_m^D, rate 1/3 convolutional encoder, interleaver, spreader and modulator according to [1,2]. n and m are discrete time. We denote the inputs to the spreader with s_n^D (DPDCH) and s_n^C (DPCCH), respectively. The output of the spreader is a code multiplexed complex chip sequence.

2.2 The time-variant mobile radio channel

At the receive antenna multiple waves are superimposed. The RAKE receiver can separate signal components with relative delays greater than one chip duration $T_C = 260\,\text{ns}$. A set of Z non-separable waves is referred to as a finger. The channel model used for simulation consists of 4 fingers. The propagation conditions are defined in [3] and given in **Table 1**.
A statistical discrete-time model of the time-variant impulse response $h_j(\tau, t)$ at the output of one RAKE-finger j with delay τ_j can be described according to [4] as

Relative path delay [ns]	0	260	521	781
Average attenuation [dB]	0	3	6	9

Table 1: Propagation conditions of the multipath fading channel

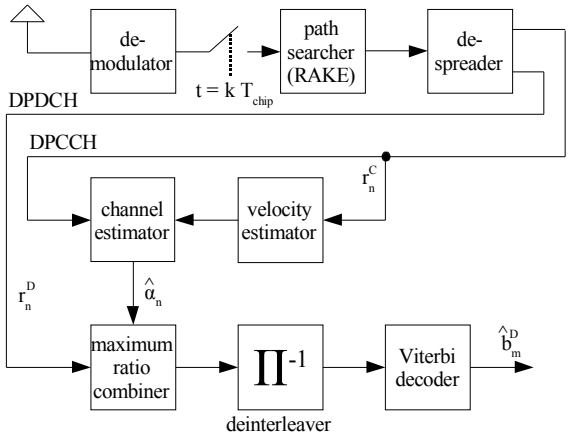

Figure 2: Block diagram of a Node B receiver with velocity estimation

$$h_j(\tau,t)=\lim_{Z\to\infty}\frac{1}{Z}\sum_{m=1}^{Z}e^{j\Theta_m}e^{j2\pi f_{D_m}t}\delta(\tau-\tau_j) \quad (1)$$

This assumes ideal correlation properties of the RAKE receiver. (1) represents the Rayleigh fading of a frequency-flat fading channel [5], where the phase-shifts Θ_m and Doppler-shifts f_{D_m} are randomly chosen according to their probability density functions $p_\Theta(\Theta)$ and $p_{f_D}(f_D)$, respectively. Θ_m is equally distributed. For the Doppler power spectrum $P(f_D)$ a Jakes-distribution is assumed, which models isotropic scattering [4].

$$P(f_D)=\frac{1}{\pi f_{D_{\max}}\sqrt{1-(f_D/f_{D_{\max}})^2}} \quad (2)$$

$f_{D_{\max}}=f_c v/c$ is the maximum Doppler frequency depending on the carrier frequency f_c and the mobile terminal speed v.

The received signal of a simplified channel model including spreading, despreading, filtering and sampling is given as $r_n=\alpha_n s_n+n_n$, where n is discrete time. A sent bit is represented by s_n, and n_n is superimposed AWGN. α_n is referred to as channel coefficient. According to (1), we assume $|\alpha_n|$ to be Rayleigh distributed.

2.3 Receiver

The investigated Node B receiver is depicted in **Figure 2**. Only one RAKE finger is illustrated. In general, the path searcher provides one sequence of complex chips per detected finger. We assume ideal path searching, i.e. the RAKE receiver finds the right number of fingers and their delays τ_j. The despreader separates the samples

$$r_n^D=\alpha_n s_n^D+n_n \text{ (DPCCH) and} \quad (3a)$$

$$r_n^C=\alpha_n s_n^C+n_n \text{ (DPCCH).} \quad (3b)$$

r_n^C are input to the channel estimator that provides estimates $\hat{\alpha}_n$ of the channel coefficients α_n. The maximum ratio combiner compensates the channel and adds all finger signals that were detected by the path searcher. After deinterleaving and Viterbi decoding estimates $\hat{b}_m^D$ of the sent bit sequence b_m^D are available.

In parallel the samples r_n^C are evaluated by the velocity estimator. The result is provided to the channel estimator, which adapts its parameters according to the detected speed.

3 Channel estimation

At the receiver the channel coefficients are estimated for each path separately. As shown before, a pilot bit s_n^C is affected by the Rayleigh fading coefficient α_n. Moreover, additive white Gaussian noise (AWGN) n_n is superimposed.

As the pilot bits $s_n^C\in\{\pm1\}$ are known at the receiver we can find estimates $\hat{\alpha}_n$ of α_n as

$$\hat{\alpha}_n=\frac{1}{N}\sum_{h=n-N_b}^{n+N_f}r_h^C s_h^C=\sum_{h=n-N_b}^{n+N_f}\alpha_h+\frac{1}{N}\sum_{h=n-N_b}^{n+N_f}n_h s_h^C, \quad (4)$$

where $N=N_b+N_f$ is the number of considered pilot bits. N_b samples are taken from the past and N_f from the future.

As n_n has zero mean, the impact of noise on the estimates can be reduced by averaging over several values $r_n^C s_n^C$ (large N). However, the channel coefficients α_n are time-variant. Thus N has also to be determined due to the rate of change of the channel. Of course this rate is related to the speed of the mobile terminal.

Under consideration of the slot based transmission in UMTS (4) can be extended to the Weighted-Multi-Slot-Averaging (WMSA) algorithm. Only one channel estimate $\hat{\alpha}_i$ for the slot i is determined as

$$\hat{\alpha}_i=\frac{1}{\sum_{g=i-4}^{i+4}w_g}\sum_{g=i-4}^{i+4}w_g\frac{1}{N_P}\sum_{m=1}^{N_P}r_{g,m}^C s_{g,m}^C. \quad (5)$$

w_i is a weighting factor for the slot i. It allows to weight contributions near to the actual slot i stronger than others. Thus, the impact of the time-variance of $\alpha_n$on the estimate $\hat{\alpha}_i$ is reduced. One DPCCH slot consists of N_P pilot symbols and $10-N_P$ non-pilot symbols. $r_{g,m}^C=r_n^C$ with $g=\lfloor n/10\rfloor$ and $m=n \bmod 10$. $\lfloor\rfloor$ denotes rounding towards the nearest smaller integer. (5) considers that at most nine slots are averaged. i addresses the actual slot, $i-4\ldots i-1$ are past slots and $i+1\ldots i+4$ are future slots. This look ahead is possible, because the DPCCH slot $i+4$ and DPDCH slot i are processed at the same time due to an artificial delay of the DPDCH.

Applying WMSA, the total number N of considered pilot symbols is given as $N = k\,N_P$, where k is the number of slots with $w_i \neq 0$.

Test Case (Speed)	N [1)]	w_i [2)]
Case 1 (3 km/h)	54 (9 slots)	[0.5 0.6 0.7 0.8 **1.0** 0.9 0.8 0.7 0.6]
Case 5 (50 km/h) [3)]	54 (7 slots)	[0.2 0.4 0.6 0.8 **1.0** 0.9 0.7 0.5 0.3]
Case 3 (120 km/h)	30 (5 slots)	0.1 0.6 **1.0** 0.9 0.3]
Case 4 (250 km/h)	12 (2 slots)	[**1.0** 0.3]

Table 2: Improved window size N and slot weights w_i for WMSA channel estimation

1) The simulation was carried out with $N_P = 6$ pilot symbols s_n^C per slot. However, [2] provides pilot patterns varying from 3 to 8 pilots per slot.

2) The central element for the actual slot is highlighted with bold font.

3) *Case 5* is not defined in [3]. It is equivalent to *Case 3* with velocity 50 km/h.

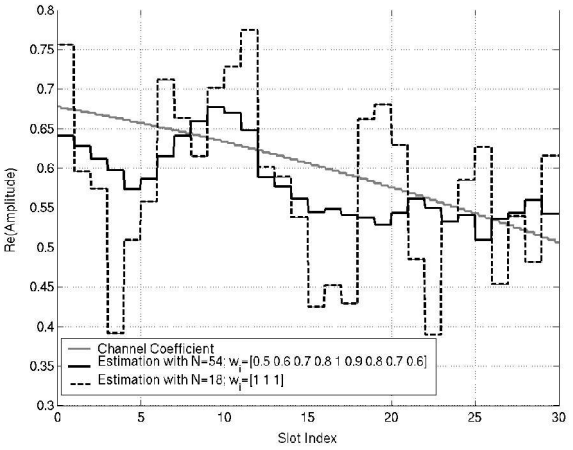

Figure 3: Channel coefficient and channel estimates for $v = 3\,\mathrm{km/h}$

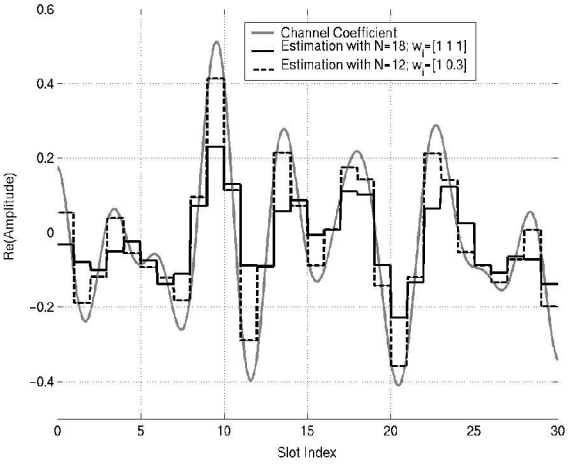

Figure 4: Channel coefficient and channel estimates for $v = 250\,\mathrm{km/h}$

We have investigated this important interrelation to find out appropriate values N and w_i for some given test cases [3]. The results are presented in **Table 2**.

The impact of N and w_i on $\hat{\alpha}_i$ is shown in two examples with speeds $v = 3\,\mathrm{km/h}$ (**Figure 3**) and $v = 250\,\mathrm{km/h}$ (**Figure 4**). Both diagrams illustrate the normalized real parts of the channel state (α_n) and channel estimates ($\hat{\alpha}_i$) during 30 slots.

For the low speed case in Figure 3 we set the signal-to-noise ratio to $E_b/N_0 = 5\,\mathrm{dB}$. During the observation time the channel coefficient α_n (gray line) is changing very slowly. Thus, the quality of the estimates $\hat{\alpha}_i$ is basically affected by the noise n_n. The estimates $\hat{\alpha}_i$ with $N = 54$ (black solid line) provide a better approximation than those with $N = 18$ (black dotted line), because the impact of the noise n_n on $\hat{\alpha}_i$ is reduced more effectively.

Figure 4 shows the high speed case without AWGN. During the observation time several deep fades occur. The channel coefficient α_n (gray line) is changing fast. Now, the channel estimates $\hat{\alpha}_i$ with $N = 12$ (black solid line) consistently provide the better result in comparison to $\hat{\alpha}_i$ with $N = 18$ (black dotted line). A small WMSA window yields a better tracking of fast changing channel conditions.

We have shown, that a compromise between noise reduction and channel tracking has to be found. The knowledge of the speed of the mobile terminal can help to set the parameters N and w_i appropriately.

4 Velocity estimation

For an estimation of the velocity the spectrum of a set of collected DPCCH pilot samples $r_{i,n}^C s_{i,n}^C$ is evaluated. Firstly values for the non-pilot symbols of the DPCCH slot i have to be determined by a linear interpolation between $r_{i,N_P}^C s_{i,N_P}^C$ and $r_{i+1,1}^C s_{i+1,1}^C$.

$$\Delta = r_{i+1,1}^C s_{i+1,1}^C - r_{i,N_P}^C s_{i,N_P}^C \tag{6}$$

$$r_{i,N_P+1}^C s_{i,N_P+1}^C = r_{i,N_P}^C s_{i,N_P}^C + \Delta/(11 - N_P)$$

$$\ldots \tag{7}$$

$$r_{i,10}^C s_{i,10}^C = r_{i,N_P}^C s_{i,N_P}^C + (10 - N_P)\Delta/(11 - N_P)$$

Thus, equally spaced samples in the time domain are available. Best results are obtained with a vector size of $2^{14} = 16384$ samples. This complies with an observation time of about 1 s. In the following, we will denote the autocorrelation function of $r_{i,n}^C s_{i,n}^C$ as x_n. **Figure 5** shows the not normalized power density spectrum $X_k = F(x_n)$, where $F(x_n)$ denotes the Discrete Fourier Transform (DFT) of x_n. The velocity was set to $v = 120\,\mathrm{km/h}$. This corresponds to the maximum Doppler frequency $f_{D_{\max}} \approx 220\,\mathrm{Hz}$. Obviously, X_k has peaks at $\pm f_{D_{\max}}$. The reason is the assumed isotropic scattering model with Jakes-distribution of the Doppler power spectrum.

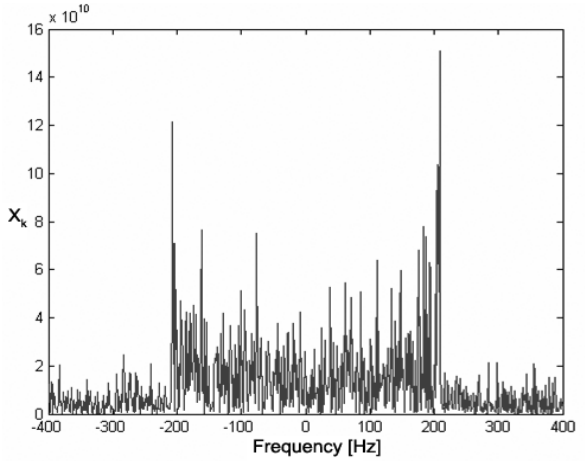

Figure 5: Power density spectrum X_k at $v = 120\,\mathrm{km/h}$

Velocity Class	Related speed $\hat{V}_i$ [km/h]	WMSA vector w_i
Low	$0 \le \hat{V}_i < 10$	[1 1 1 **1** 1 1 1 1]
Medium	$10 \le \hat{V}_i < 60$	[0.25 0.5 0.75 1 0.75 0.5 0.25]
Fast	$60 \le \hat{V}_i < 130$	[0.4 0.6 **1** 0.8 0.5]
Very fast	$\hat{V}_i \ge 130$	[0.4 **1** 0.5]

Table 3: Definition of velocity classes to find an appropriate WMSA weighting vector w_i

However, velocity estimation is not limited to the used channel model. $\pm f_{D_{\max}}$ can also be detected in a differently shaped spectrum X_k. Thus, an estimate $\hat{f}_{D_{\max}}$ of the maximum Doppler frequency is given as

$$\hat{f}_{D_{\max}} = f(\max\{X_k\}), \tag{8}$$

where $f(X_l)$ is the frequency that corresponds to the sample X_l out of the set X_k. The related estimate of the velocity $\hat{v}_i$ in slot i can be determined as

$$\hat{v}_i = c\,\hat{f}_{D_{\max}} / f_c \tag{9}$$

The estimation of the velocity may be erroneous in the presence of noise. To overcome this problem the mean value $\hat{V}_i$ over estimates $\hat{v}_i$ from previous slots is considered.

$$\hat{V}_i = \frac{1}{N_S} \sum_{k=i-N_S+1}^{i} \hat{v}_i. \tag{10}$$

Appropriate values for N_S were found to be $1000 \ldots 10000$. If the speed of the mobile terminal is changing fast, N_S has to be small and vice versa.

As the WMSA parameters N and w_i were only optimized for the the speeds $v = 3, 50, 120$ and $250\,\mathrm{km/h}$, we define the four velocity classes for low, medium, fast and very fast speed in **Table 3**. N and w_i are adapted according to the velocity class of the estimate $\hat{V}_i$.

Time [s]	0 - 1.2	1.2 - 2.4	2.4 - 3.6	3.6 -5
Speed [km/h]	3	50	120	50

Table 4: Speed profile used for simulation

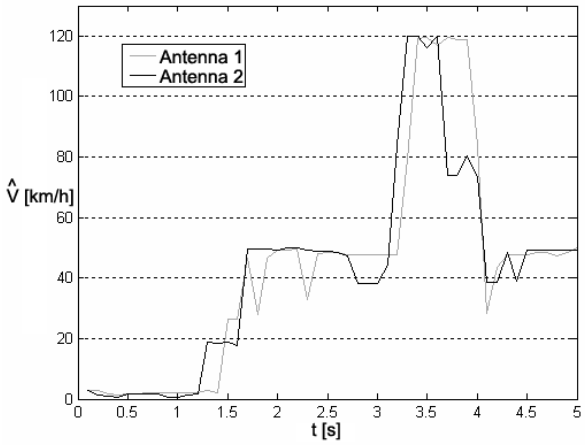

Figure 6: Estimates $\hat{V}_i$ of the speed detected from the signals of two uncorrelated receive antennas

5 Performance Evaluation

We compare our receiver with velocity estimation and adaptive channel estimation to the conventional method. For simulation we use the 3GPP reference measurement channel with 12.2 kbps DPDCH bitrate and spreading factor 64 as defined in [3]. The power ratio of DPCCH and DPDCH is $\gamma = -2.69\,\mathrm{dB}$. Of course, 12.2 kbps are not sufficient for high quality video. However, the described algorithm is still feasible, because it is based on DPCCH, which is independent from the bitrate of the data channel DPDCH. As is well known, bitrate in DPDCH can range up to 2.048 Mbps. Thus, the following results are qualitatively but not quantitatively transferable to higher bitrates.

During the simulation the speed profile in **Table 4** is passed through periodically. **Figure 6** shows $\hat{V}_i$ during one period of the speed profile. As our receiver exploits space diversity, the values $\hat{V}_i$ obtained from two receive antennas are recorded. Obviously, our algorithm estimates the speed sufficiently precisely. The few mismatches will not degrade the performance severely. The reason for the delay is that eq. (10) also takes information from the past. However, in reality the velocity will change more slowly than the profile in Table 4 does. Thus, in reality we expect even better results.

Finally, BLER of our receiver is compared to a receiver that uses constant WMSA parameters $N = 18$ (3 slots) and $w_i = [1\,1\,1]$. These values were found as an adequate compromise for both low and high speed. **Figure 7** shows the BLERs of both receivers for different signal-to-noise ratios E_b / N_0. Obviously, the receiver with velocity estimation and adaption of N and w_i is superior to the conventional method.

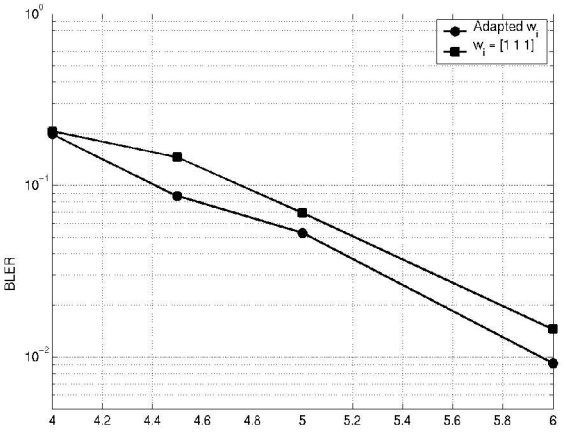

Figure 7: BLER of the proposed method in comparison to the conventional receiver

At a BLER of 10% the proposed method yields a gain of 0.3 dB. Thus, the proposed velocity estimation and adaption of the WMSA weighting vector w_i improves receiver performance.

6 Conclusion

Channel estimation becomes a crucial issue, if the mobile terminal is moving fast. On the other hand applications like video which require low BLER suffer from bad estimation of the time-variant mobile radio channel with multiple paths. We have shown that the observation time of the channel and the slot weighting factors have significant impact on the quality of the estimates. Optimal values of these parameters for several speeds were found out.
Starting from a conventional Node B receiver without adaption of the channel estimation parameters, we have presented a receiver with velocity estimation. By evaluating the spectrum of collected received pilots, the maximum Doppler frequency and consequently the speed of the mobile terminal can be determined.
This method was investigated with the Jakes-distributed Doppler power spectrum, but it is not limited to this model. Simulation results show, that our algorithm can estimate the velocity very precisely. Even the challenge of fast changing speeds does not degrade the performance considerably.
Finally, we have compared our solution with a conventional receiver without velocity estimation and constant WMSA parameters. It was found that the improved receiver yields a 0.3dB performance improvement compared to the conventional method at BLER 10%. Thus, the proposed algorithm is a promising candidate for beyond 3G systems, that improves or even enables high quality reception of video in moving vehicles.

Acknowledgment

For simulations we used an extended version of a Node B link level simulator by Alcatel Stuttgart. Some functions of the software were implemented by T. Hof during his Study Thesis.

References

[1] 3GPP: "25.212 - Multiplexing and channel coding (FDD)", *Technical specification for Release 1999*, version 3.11.0, 2002.
[2] 3GPP: "25.213 - Spreading and modulation (FDD)", *Technical specification for Release 1999*, version 3.8.0, 2002.
[3] 3GPP: "25.141 - Base Station (BS) conformance testing (FDD)", *Technical specification for Release 1999*, version 3.13.0, 2003.
[4] P. Höher: "A statistical discrete-time model for the WSSUS multipath channel", *IEEE Transactions on Vehicular Technology*, vol. 41, pp. 461-468, November 1992.
[5] B. Sklar: "Rayleigh fading channels in mobile digital communication systems - Part I: Characterization", *IEEE Communications Magazine*, vol. 35, pp. 148-155, September 1997.